

# Production of excited electrons at TESLA and CLIC based $e\gamma$ colliders

Z. Kırca<sup>a</sup>, O. Çakır<sup>b</sup> and Z.Z. Aydın<sup>c</sup>

<sup>a</sup>*Osmangazi University, Faculty of Arts and Sciences,*

*Department of Physics, 26480, Meselik, Eskişehir, Turkey.*

<sup>b</sup>*Ankara University, Faculty of Sciences,*

*Department of Physics, 06100, Tandoğan, Ankara, Turkey.*

<sup>c</sup>*Ankara University, Faculty of Engineering,*

*Department of Engineering Physics, 06100, Tandoğan, Ankara, Turkey.*

## Abstract

We analyze the potential of TESLA and CLIC based electron-photon colliders to search for excited spin-1/2 electrons. The production of excited electrons in the resonance channel through the electron-photon collision and their subsequent decays to leptons and electroweak gauge bosons are investigated. We study in detail the three signal channels of excited electrons and the corresponding backgrounds through the reactions  $e\gamma \rightarrow e\gamma$ ,  $e\gamma \rightarrow eZ$  and  $e\gamma \rightarrow \nu W$ . Excited electrons with masses up to about 90% of the available collider energy can be probed down to the coupling  $f = f' = 0.05(0.1)$  at TESLA(CLIC) based  $e\gamma$  colliders.

## I. INTRODUCTION

In order to explain the fundamental aspects of the standard model (SM) such as the number of fermion generations and fermion mass spectrum compositeness models are expected to be a good candidate. The replication of three fermionic generations of known quarks

and leptons implies composite structures made up of more fundamental constituents. The existence of such quark and lepton substructure leads one to expect a rich spectrum of new particles with unusual quantum numbers. A possible signal of excited states of quarks and leptons as predicted by composite models [1,2] would supply convincing evidence for a new substructure of matter. All composite models of fermions have an underlying substructure which is characterized by a scale  $\Lambda$ . In such models, the known light fermions would be the ground state spectrum of the excited fermions.

In order to have an agreement between the precise measurements of electron and muon  $g - 2$  and theoretical predictions for chiral couplings, the compositeness scale  $\Lambda$  is expected to be less than 10 TeV [3]. The absence of electron and muon electric dipole moments implies the chiral properties of the excited leptons. A right-handed excited lepton should couple to only left-handed components of the corresponding lepton. Excited leptons may be classified by  $SU(2) \times U(1)$  quantum numbers and they are assumed to be both left- and right-handed weak isodoublets.

Experimental lower limits for the excited electron mass are given as  $m_\star > 200$  GeV in [4], and  $m_\star > 306$  GeV in [5]. The higher limits are derived from indirect effects due to  $e^\star$  exchange in the t-channel and depend on transition magnetic coupling between  $e$  and  $e^\star$ . Relatively small limits ( $m_{\mu^\star, \tau^\star} > 94.2$  GeV) for excited muon ( $\mu^\star$ ) and excited tau ( $\tau^\star$ ) are given by the LEP L3 experiment [6].

Excited leptons have been studied at  $\gamma\gamma$  and  $e\gamma$  colliders [7],  $e^+e^-$  colliders [8], [9], and hadron colliders [10].

In this work, resonant production of excited electron in the s-channel and its subsequent decay modes  $e^\star \rightarrow e\gamma$ ,  $e^\star \rightarrow \nu W$ ,  $e^\star \rightarrow eZ$  are considered. In addition, we include the contributions coming from the excited electron in the t-channel. In order to probe excited electrons, we examine the potential of TESLA and CLIC based  $e\gamma$  colliders with the main parameters given in Table I. The production cross section and decays of excited electrons are calculated using an effective Lagrangian which depends on a compositeness scale  $\Lambda$  and on free parameters  $f$  and  $f'$ .

## II. EFFECTIVE LAGRANGIAN

The Lagrangian describing the transition between ordinary and excited leptons should respect to chiral symmetry in order to protect the light leptons from acquiring radiatively a large anomalous magnetic moment. The excited leptons ( $l^*$ ) can couple to leptons ( $l$ ) and electroweak gauge bosons through the  $SU(2) \times U(1)$  invariant effective interaction Lagrangian [2]

$$L = \frac{1}{2\Lambda} \bar{l}^* \sigma_{\mu\nu} \left( g f \frac{\tau}{2} \cdot W_{\mu\nu} + g' f' \frac{Y}{2} B_{\mu\nu} \right) l_L + \text{H.c.} \quad (1)$$

where the  $W_{\mu\nu}$  and  $B_{\mu\nu}$  represent the field strength tensors of  $SU(2)$  and  $U(1)$  gauge fields. The  $\tau$  and  $Y$  are the corresponding gauge group generators;  $g$  and  $g'$  are gauge coupling constants. The parameters  $f$  and  $f'$  associated to the gauge groups  $SU(2)$  and  $U(1)$  depend on compositeness dynamics and they describe the effective changes from the SM coupling constants  $g$  and  $g'$ . In the physical basis the Lagrangian (1) can be rewritten in more explicit form

$$L = \frac{g_e}{2\Lambda} \left[ (f - f') N_{\mu\nu} \sum_{l=e,\nu} \bar{l}^* \sigma^{\mu\nu} l_L + f \sum_{l,l'=e,\nu} \Theta_{\mu\nu}^{\bar{l}^*,l} \bar{l}^* \sigma^{\mu\nu} l'_L \right] + \text{H.c.} \quad (2)$$

where the first term in the paranthesis is a purely diagonal  $U(1)$  term and vanishes for the coupling  $f = f'$ . It contains only triple vertices with

$$N_{\mu\nu} = \partial_\mu A_\nu - \tan \theta_W \partial_\mu Z_\nu. \quad (3)$$

The second term in (2) is a non-abelian part which involves triple as well as quartic terms with

$$\Theta_{\mu\nu}^{\bar{\nu}^*,\nu} = \frac{1}{\cos \theta_W \sin \theta_W} \partial_\mu Z_\nu - i \frac{g_e}{\sin^2 \theta_W} W_\mu^+ W_\nu^- \quad (4)$$

$$\Theta_{\mu\nu}^{\bar{e}^*,e} = - \left( 2\partial_\mu A_\nu + \frac{\cos^2 \theta_W - \sin^2 \theta_W}{\cos \theta_W \sin \theta_W} \partial_\mu Z_\nu - i \frac{g_e}{\sin^2 \theta_W} W_\mu^+ W_\nu^- \right) \quad (5)$$

$$\Theta_{\mu\nu}^{\bar{\nu}^*,e} = \frac{\sqrt{2}}{\sin \theta_W} \left( \partial_\mu W_\nu^+ - i g_e W_\mu^+ (A_\nu + \cot \theta_W Z_\nu) \right) \quad (6)$$

$$\Theta_{\mu\nu}^{\bar{e}^*,\nu} = \frac{\sqrt{2}}{\sin \theta_W} \left( \partial_\mu W_\nu^- + i g_e W_\mu^- (A_\nu + \cot \theta_W Z_\nu) \right). \quad (7)$$

From Eq. (2), the vertex factor for excited lepton ( $l^*$ ) interacting with lepton ( $l$ ) and gauge bosons ( $V = \gamma, Z, W$ ) can be obtained as follows

$$\Gamma_\mu^{V l^* l} = \frac{g_e}{2\Lambda} q^\nu \sigma_{\mu\nu} (1 - \gamma_5) f_V \quad (8)$$

where  $q$  is the gauge boson momentum. The couplings  $f_V$  are defined by

$$f_\gamma = Q_f f' + I_{3L} (f - f') \quad (9)$$

$$f_W = \frac{f}{\sqrt{2} \sin \theta_W} \quad (10)$$

$$f_Z = \frac{-Q_f \sin^2 \theta_W f' + I_{3L} (\cos^2 \theta_W f + \sin^2 \theta_W f')}{\cos \theta_W \sin \theta_W} \quad (11)$$

where  $Q_f$  and  $I_{3L}$  are the charge of excited lepton and the weak isospin, respectively; and  $\theta_W$  is the weak mixing angle.

### III. DECAY WIDTHS

Decay widths of excited electrons in the individual channels  $e^* \rightarrow e\gamma$ ,  $e^* \rightarrow eZ$ , and  $e^* \rightarrow \nu W$  are given by

$$\Gamma(e^* \rightarrow e\gamma) = \frac{\alpha}{4} \frac{m_\star^3}{\Lambda^2} f_\gamma^2 \quad (12)$$

$$\Gamma(e^* \rightarrow eZ) = \frac{\alpha}{4} \frac{m_\star^3}{\Lambda^2} f_Z^2 \left(1 - \frac{m_Z^2}{m_\star^2}\right)^2 \left(1 + \frac{m_Z^2}{2m_\star^2}\right) \quad (13)$$

$$\Gamma(e^* \rightarrow \nu W) = \frac{\alpha}{4} \frac{m_\star^3}{\Lambda^2} f_W^2 \left(1 - \frac{m_W^2}{m_\star^2}\right)^2 \left(1 + \frac{m_W^2}{2m_\star^2}\right). \quad (14)$$

For  $m_\star \gg m_{Z,W}$ , total decay width of excited electron is given by

$$\Gamma_{tot} \simeq \frac{\alpha}{4} \frac{m_\star^3}{\Lambda^2} [f_\gamma^2 + f_W^2 + f_Z^2] \quad (15)$$

The branching ratios for the excited electron decay channels are described as follows

$$BR = \frac{\Gamma(e^* \rightarrow lV)}{\sum_V \Gamma(e^* \rightarrow lV)}. \quad (16)$$

where  $l$  is electron or neutrino. We choose the parameters either  $f = f'$  or  $f = -f'$  in our calculations in order to reduce the number of free parameters. For the case  $f = f'$  ( $f = -f'$ ) the coupling of the photon to excited neutrinos (electrons) vanishes. We display the decay widths and branching ratios for excited electrons in Fig. 1. The decay widths of excited electrons, for the accessible mass range, could be comparable with the detector resolution at TESLA and CLIC based  $e\gamma$  colliders. As can be seen from Fig. 1 an excited electron decays into a W boson and a neutrino dominantly, and the branching ratios are insensitive to higher excited electron mass when compared to  $m_W$  or  $m_Z$ . We obtain the limiting values for the branching ratios at large  $m_\star$  as 0.28, 0.60 and 0.11 for the coupling  $f = f' = 1$  at photon, W and Z channel, respectively. In the case  $f = -f' = -1$ , the branching ratio for W channel does not change while it increases to the value 0.39 for Z channel.

#### IV. CROSS SECTIONS

Excited electrons can be produced directly via the subprocess  $e\gamma \rightarrow e^\star \rightarrow lV$  ( $V = \gamma, Z, W$ ) and indirectly via t-channel exchange diagram. The Feynman diagrams for  $e\gamma \rightarrow e\gamma(eZ)$  and  $\gamma e \rightarrow \nu W$  processes in electron-photon collisions are shown in Fig. 2 and 3.

For an immediate estimation, the cross section for the signal can be well approximated with the Breit Wigner formula

$$\hat{\sigma}_{BW} = \frac{8\pi^2 \Gamma_i \cdot \Gamma_f}{m_\star s \Gamma_{tot}} f_\gamma(x) \quad (17)$$

for the narrow decay widths where  $\Gamma_i$  and  $\Gamma_f$  are the initial and final state decay widths, respectively. Here,  $x = \hat{s}/s$  where  $\sqrt{\hat{s}}$  being the center of mass energy of the subprocess. In order to obtain the total cross sections for the signal and background, without the narrow width approximation, we use the following formula

$$\sigma = \int_{x_{\min}}^{0.83} dx f_\gamma(x) \hat{\sigma}(\hat{s}). \quad (18)$$

where  $\hat{\sigma}(\hat{s})$  is obtained from the well-known matrix element calculation from the Feynman

diagrams given in Figs. 2 and 3. Here,  $x_{\min} = m_\star^2/s$ . The high energy photon spectrum  $f_\gamma(x)$  obtained from the Compton backscattering is given by

$$f_\gamma(x) = \begin{cases} \frac{1}{N} \left[ 1 - x + \frac{1}{1-x} \left[ 1 - \frac{4x}{x_0} \left( 1 - \frac{x}{x_0(1-x)} \right) \right] \right] & , 0 < x < x_{\max} \\ 0 & , x > x_{\max} \end{cases} \quad (19)$$

where  $x_0 = 4.82$ ,  $x_{\max} = x_0/(1 + x_0)$  and  $N=1.84$  [11]. The production cross section of excited electron in three modes, taking  $f = f' = 1$  and  $\Lambda=m_\star$ , are given in Fig. 4 and 5 for TESLA and CLIC based  $e\gamma$  colliders at the center of mass energies of  $\sqrt{s} = 911$  GeV and  $\sqrt{s} = 2733$  GeV, respectively. From Fig. 4 and Fig. 5, we get the following information; the  $\nu W$  channel gives higher cross section than the others however there is an ambiguity with the neutrino in this channel. Therefore, the photon channel gives a more promising result because of its simple kinematics. Excited electrons can be produced copiously at TESLA and CLIC based  $e\gamma$  colliders. The cross sections and the numbers of signal events are shown in Table II and III. For the signal and background processes we apply a cut  $p_T^{e,\gamma} > 10$  GeV for experimental identification of final state particles. The backgrounds to the W and Z decay channels in the hadronic final states are fairly large. The backgrounds to the photonic final states are relatively small in comparasion with the W channels.

In order to get one particle inclusive cross sections for the production of a particle of transverse momentum  $p_T$  and rapidity  $y$ , we use the following standard procedure. The differential cross section for the process  $e\gamma \rightarrow eZ$  with respect to the transverse momentum  $p_T$  of outgoing electron is given by

$$\frac{d\sigma}{dp_T} = 2p_T \int_{y^-}^{y^+} dy f_{\gamma/e}(x) \frac{xs}{|s - 2p_TE_a e^{-y}|} \frac{d\hat{\sigma}}{d\hat{t}} \quad (20)$$

with

$$x = \frac{2p_TE_b e^y + m_Z^2}{s - 2p_TE_a e^{-y}}$$

and

$$y^\pm = \log \left[ \frac{0.83s - m_Z^2}{4p_TE_b} \pm \sqrt{\left( \frac{0.83s - m_Z^2}{4p_TE_b} \right)^2 - \frac{0.83E_a}{E_b}} \right]$$

where  $E_a$  and  $E_b$  are the incoming particle energies.  $\hat{s}$  and  $\hat{t}$  are the Lorentz invariant Mandelstam variables.

The  $p_T$  distribution of  $W$  boson in  $e\gamma$  collision at rapidity  $y$  for the process  $e\gamma \rightarrow \nu W$  is given by

$$\frac{d\sigma}{dp_T} = 2p_T \int_{y^-}^{y^+} dy f_\gamma(x) \left| \frac{xs}{s - 2m_T E_a e^{-y}} \right| \frac{d\hat{\sigma}}{d\hat{t}} \quad (21)$$

with

$$x = \frac{2m_T E_b e^y - m_W^2}{s - 2m_T E_a e^{-y}}$$

and

$$y^\pm = \log \left[ \frac{0.83s + m_W^2}{4m_T E_b} \pm \sqrt{\left( \frac{0.83s + m_W^2}{4m_T E_b} \right)^2 - \frac{0.83E_a}{E_b}} \right]$$

where  $m_T = \sqrt{m_W^2 + p_T^2}$  is the definition for the transverse mass of  $W$  boson.

The production of a photon in  $e\gamma$  collision at rapidity  $y$  and transverse momentum  $p_T$  for the process  $e\gamma \rightarrow e\gamma$  can be found by replacing  $m_W = 0$  in (21).

In the Eqs. (20) and (21), we have calculated the differential cross sections  $d\hat{\sigma}/d\hat{t}$  for the signal and background processes taking into account the interferences between the SM and excited electrons contributions.

For both signal and background, the behavior of  $p_T$  spectrum of final state photon,  $W$  boson and electron in three modes are shown in Figures 6-8 for various values of parameters  $f = f'$  at TESLA based  $e\gamma$  collider with  $\sqrt{s} = 911$  GeV. At CLIC based  $e\gamma$  collider with  $\sqrt{s} = 2733$  GeV, we can easily scale the cross sections according to Figs. 4 and 5. For signal process  $e\gamma \rightarrow e^* \rightarrow e\gamma$ , transverse momentum  $p_T$  distribution of photon or electron is peaked around the half of the mass value of excited electron. For the process  $e\gamma \rightarrow e^* \rightarrow \nu W(eZ)$ ,  $p_T$  distribution of  $W$  boson (electron) shows a peak around  $m_*/2 - m_V^2/2m_*$ . Here  $m_V$  denotes  $W$  boson (or  $Z$  boson) mass. This signal peak moves to a greater (smaller)  $p_T$  value when the excited electron mass increased (decreased). For the parameters  $f = f' \neq 1$  one

can conclude that the  $p_T$  distribution changes simply with  $f^2$ . The backgrounds decrease smoothly when the transverse momentum of final state particles increase.

In order to estimate the number of events for the signal and background in a chosen  $p_T$  window, we integrate the transverse momentum distribution around the half of each excited electron mass point  $(m_\star/2 - m_V^2/2m_\star)$  in the interval of transverse momentum resolution  $\Delta p_T$ . Here  $\Delta p_T$  is approximated as  $\approx 10$  GeV for  $m_\star = 500$  GeV and  $\approx 20$  GeV for  $m_\star = 1500$  GeV for a generic detector. In order to calculate signal significance, we use the integrated luminosity for TESLA and CLIC based  $e\gamma$  colliders with  $L = 9.4 \times 10^4 \text{ pb}^{-1}$  and  $L = 9 \times 10^4 \text{ pb}^{-1}$ , respectively [12].

In order to quantify the potential of TESLA and CLIC based  $e\gamma$  colliders to search for excited electron, we define the statistical significance (SS)

$$SS = \frac{|\sigma_{total} - \sigma_{back}|}{\sqrt{\sigma_{back}}} \sqrt{L}. \quad (22)$$

where  $\sigma_{total}$  and  $\sigma_{back}$  is the total cross sections for signal+background and background inside chosen  $p_T$  window, respectively. We calculate the value of SS for different couplings assuming  $f = f'$  and requiring the condition  $SS > 5$  for the signal observability. We find from the Tables IV-VII that the excited electrons can be observed down to coupling  $f \simeq 0.05$  at TESLA and  $f \simeq 0.1$  at CLIC based  $e\gamma$  colliders.

In the final states containing W or Z boson we should consider the subsequent decay modes of the weak bosons. For leptonic decay the branching ratios are  $BR(W \rightarrow l\nu) \cong 10.56\%$  and  $BR(Z \rightarrow l^+l^-) \cong 3.37\%$ . However hadronic decay modes have larger branchings as  $BR(W \rightarrow \text{Hadrons}) \cong 68.5\%$  and  $BR(Z \rightarrow \text{Hadrons}) \cong 69.89\%$  [13]. We should multiply the cross sections for  $2 \rightarrow 2$  processes by the branching ratios for subsequent decays of W or Z boson in the weak decay channels of excited electron. Here we do not consider the invisible decay modes. The direct production of excited electrons at  $e\gamma$  collider will give the signal in the final state a) electron+photon or b) lepton+ $p_T^{miss}$  or c) 2jet+ $p_T^{miss}$



or d) electron+2lepton or e)electron+ $p_T^{miss}$  or f) electron+ 2jet. For the observation of more clear signal we may choose the leptonic channels.

## V. RESULTS AND DISCUSSIONS

Excited electrons can be produced directly with a large cross section (even in the three decay modes) at high energy TESLA and CLIC based  $e\gamma$  colliders. For an observation, we require the condition  $SS > 5$  per year at  $e\gamma$  colliders with the integrated luminosity of  $O(\sim 10^5 pb^{-1})$ . With the couplings  $f = f' = 1$  we can reach the excited electron mass up to the kinematical limits of collider energies. For smaller values of the parameters  $f$  and  $f'$ , the cross sections are lowered simply by  $f^2$ . If excited electrons with a lower parameters exist, we will need high resolution detectors.

In this study, we have taken into account that the excited electrons interact with the Standard Model particles through the effective Lagrangian (1). This may be a conservative assumption because it is possible for excited fermions couple to ordinary quarks and leptons via contact interactions originating from the strong constituents dynamics. In this case, the decay widths can be enhanced [14].

In conclusion, we have presented the results of excited electron production with subsequent decays into three decay channels. The excited electrons can be produced at TESLA and CLIC based  $e\gamma$  colliders up to kinematical limit at each channel due to the smooth photon energy spectrum. We find that excited electron with mass 500(750) GeV can be probed down to the coupling  $f = f' \simeq 0.05$  at TESLA based  $e\gamma$  colliders. At a CLIC based  $e\gamma$  collider ( $\sqrt{s} = 2733$  GeV), the excited electron can be probed down to the couplings  $f = f' \simeq 0.1$ .

## REFERENCES

- [1] H. Harari, Phys. Lett. 86B, 83 (1979); H. Terazawa, Phys. Rev. D 22, 184 (1980); L. Abbott and E. Farhi, Nucl. Phys. B 189, 547 (1981); H. Fritzsch and G. Mandelbaum, Phys. Lett. B 102, 319 (1981).
- [2] F. M. Renard, Phys. Lett. B 116, 264 (1982); K. Hagiwara, S. Komamiya and D. Zeppenfeld, Z. Phys. C 29, 115 (1985); U. Baur, M. Spira and P. M. Zerwas, Phys. Rev. D 42, 815 (1990); F. Boudjema, A. Djouadi and J.L. Kneur, Z. Phys. C 57, 425 (1993).
- [3] F. M. Renard, Phys. Lett. B 116, 264 (1982); F. DelAquila, A. Mendez and R. Pascual, Phys. Lett. B 140, 431 (1984); M. Suzuki, Phys. Lett. B 143, 237 (1984).
- [4] J. Breitweg *et al.*, ZEUS Collaboration, Z. Phys. C 76, 631 (1997).
- [5] G. Abbiendi *et al.*, OPAL Collaboration, Phys. Lett. B 465, 303 (1999).
- [6] M. Acciarri *et al.*, L3 Collaboration, Phys. Lett. B 353, 431 (1984).
- [7] I. F. Ginzburg, D. Yu. Ivanov, Phys. Lett. B 276, 214 (1992).
- [8] R. Kleiss, P.M. Zerwas, CERN workshop on Physics at Future Accelerators, La Thuile, 1987, vol. 2, 277.
- [9] G. Abbiendi *et al.*, OPAL Collaboration, Phys. Lett. B 544, 57 (2002).
- [10] O.J.P. Eboli, S.M. Lietti and P. Mathews, Phys. Rev. D 65, 075003 (2002).
- [11] I. F. Ginzburg, G. L. Kotkin, V. G. Serbo, V. I. Telnov, Nucl. Instr. Meth. and Math. 47, 205 (1983)
- [12] H. Abromowicz *et al.*; TESLA-N Study Group, TESLA TDR, Appendix I, Chapter-I, p 55, DESY-01-011, (2001)
- [13] D. E. Groom *et al.*, (Particle Data Group), The Eur. Phys. J. C 15, 21 (2000)
- [14] O. Çakır, C. Leroy and R. Mehdiyev, ATLAS Internal Note, ATL-PHYS-2002-014,

(2002)

# TABLES

TABLE I. Main parameters of TESLA and CLIC  $e^+e^-$  colliders and  $e\gamma$  colliders based on them.

	$\sqrt{s_{ee}}$ (GeV)	$\sqrt{s_{e\gamma}}$ (GeV)	$L_{e\gamma}(10^{34}cm^{-2}sn^{-1})$
TESLA	1000	911	0.94
CLIC	1000	911	0.35
CLIC	3000	2733	0.90

TABLE II. Cross sections and number of events for signal at  $\sqrt{s_{e\gamma}} = 911$  GeV. Here the numbers  $N_1$  and  $N_2$  are for TESLA and CLIC based  $e\gamma$  colliders, respectively.

		$e\gamma \rightarrow e\gamma$		$e\gamma \rightarrow \nu W$			$e\gamma \rightarrow eZ$		
$m_*(GeV)$	$\sigma$ (pb)	$N_1(10^2)$	$N_2(10^2)$	$\sigma(pb)$	$N_1(10^2)$	$N_2(10^2)$	$\sigma$ ( pb)	$N_1(10^2)$	$N_2(10^2)$
200	27.80	26132	9730	38.82	36491	13587	10.57	9936	3699
300	14.22	13367	4977	26.11	24543	9139	5.32	5000	1862
400	11.50	10810	4025	23.40	21996	8190	4.46	4192	1561
500	9.87	9278	3455	20.85	19599	7298	3.92	3685	1372
600	9.22	8667	3227	19.80	18612	6930	3.71	3487	1299
700	9.26	8704	3241	20.06	18856	7021	3.76	3535	1316
800	11.07	10406	3875	24.13	22682	8446	4.52	4249	1582
900	20.74	19496	7259	45.34	42620	15869	8.49	7981	2972

TABLE III. Cross sections and number of events for signal at CLIC based  $e\gamma$  collider with  $\sqrt{s} = 2733$  GeV and integrated luminosity  $L = 9 \times 10^4 \text{pb}^{-1}$ .

$m_*(\text{GeV})$	$e\gamma \rightarrow e\gamma$		$e\gamma \rightarrow \nu W$		$e\gamma \rightarrow eZ$	
	$\sigma(\text{pb})$	N( $10^2$ )	$\sigma(\text{pb})$	N( $10^2$ )	$\sigma(\text{ pb})$	N( $10^2$ )
200	197.10	177400	223.50	201200	81.74	73570
400	12.53	11280	15.52	13970	5.19	4671
600	3.07	2763	4.64	4176	1.27	1143
800	1.73	1557	3.21	2889	0.71	639
1000	1.41	1269	2.89	2601	0.58	522
1200	1.23	1107	2.63	2367	0.51	459
1400	1.11	999	2.41	2169	0.46	414
1600	1.04	936	2.28	2052	0.43	387
1800	1.01	907	2.22	1998	0.41	369
2000	1.00	903	2.21	1989	0.41	369
2200	1.05	945	2.31	2079	0.43	387
2400	1.22	1098	2.70	2430	0.50	450
2600	1.80	1620	3.98	3582	0.75	675

TABLE IV. The total cross sections of signal and backgrounds inside the bin chosen and statistical significance (SS) values according to different  $f = f'$  for  $m_* = 500$  GeV at  $\sqrt{s} = 911$  GeV with  $L = 9.4 \times 10^4 \text{pb}^{-1}$ .

$m_* = 500$ GeV						
	$e\gamma \rightarrow e\gamma$		$e\gamma \rightarrow \nu W$		$e\gamma \rightarrow eZ$	
$f = f'$	$\sigma_{tot}(\text{pb})$	$SS$	$\sigma_{tot}(\text{pb})$	$SS$	$\sigma_{tot}(\text{pb})$	$SS$
1.00	24.80	2100.4	78.00	1711.3	8.50	1758.8
0.50	11.20	508.5	50.80	422.8	3.20	424.5
0.10	7.03	19.8	41.90	3.1	1.60	16.6
0.05	6.87	0.7			1.52	2.9

TABLE V. The total cross sections of signal and background inside the bin chosen and statistical significance (SS) values according to different  $f = f'$  for  $m_* = 750$  GeV at  $\sqrt{s} = 911$  GeV with  $L = 9.4 \times 10^4 \text{pb}^{-1}$ .

$m_* = 750$ GeV						
	$e\gamma \rightarrow e\gamma$		$e\gamma \rightarrow \nu W$		$e\gamma \rightarrow eZ$	
$f = f'$	$\sigma_{tot}(\text{pb})$	$SS$	$\sigma_{tot}(\text{pb})$	$SS$	$\sigma_{tot}(\text{pb})$	$SS$
1.00	24.70	1834.8	80.10	1812.4	8.90	1847.5
0.50	11.30	455.3	51.40	452.3	3.40	673.3
0.10	7.04	18.4	42.13	12.8	1.60	23.6
0.05	6.87	0.7	41.88	1.1	1.52	3.8

TABLE VI. The total cross sections of signal and background inside the bin chosen and statistical significance (SS) values according to different  $f = f'$  for  $m_* = 750$  GeV at  $\sqrt{s} = 2733$  GeV with  $L = 9 \times 10^4 \text{pb}^{-1}$ .

$m_* = 750$ GeV						
	$e\gamma \rightarrow e\gamma$		$e\gamma \rightarrow \nu W$		$e\gamma \rightarrow eZ$	
$f = f'$	$\sigma_{tot}(\text{pb})$	$SS$	$\sigma_{tot}(\text{pb})$	$SS$	$\sigma_{tot}(\text{pb})$	$SS$
1.00	4.30	866.8	53.40	190.2	1.51	634.9
0.50	1.80	165.4	50.00	46.7	0.53	118.1
0.10	1.20	5.5	48.94	0.6	0.32	3.7
0.05	1.18	0.7				

TABLE VII. The total cross sections of signal and background inside the bin chosen and statistical significance values according to different  $f = f'$  for  $m_* = 1500$  GeV at  $\sqrt{s} = 2733$  GeV with  $L = 9 \times 10^4 \text{pb}^{-1}$ .

$m_* = 1500$ GeV						
	$e\gamma \rightarrow e\gamma$		$e\gamma \rightarrow \nu W$		$e\gamma \rightarrow eZ$	
$f = f'$	$\sigma_{tot}(\text{pb})$	$SS$	$\sigma_{tot}(\text{pb})$	$SS$	$\sigma_{tot}(\text{pb})$	$SS$
1.00	3.10	537.9	52.90	173.2	1.12	427.7
0.50	1.60	130.3	49.90	43.7	0.51	102.8
0.10	1.20	4.3	48.93	0.1	0.32	2.8

# FIGURES

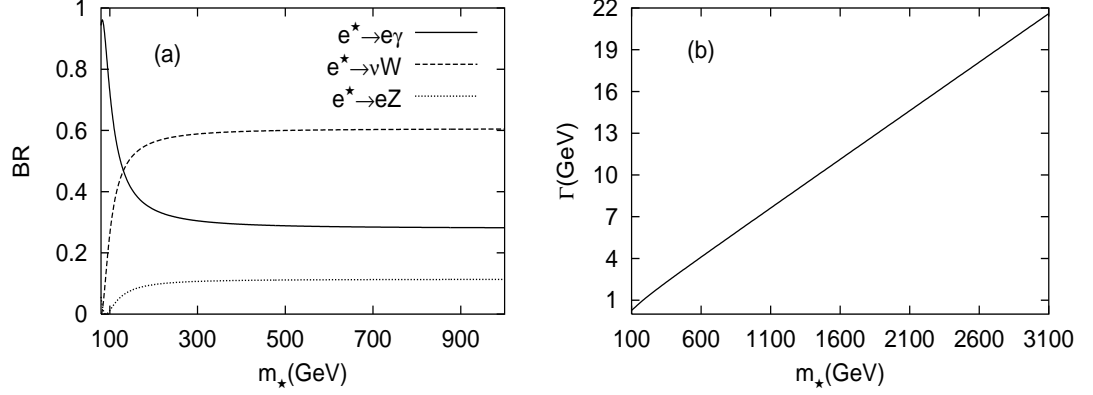


FIG. 1. The branching ratios (a) and the total decay width (b) for excited electrons as a function of its mass with  $\Lambda = m_*$  and the coupling  $f = f' = 1$ .

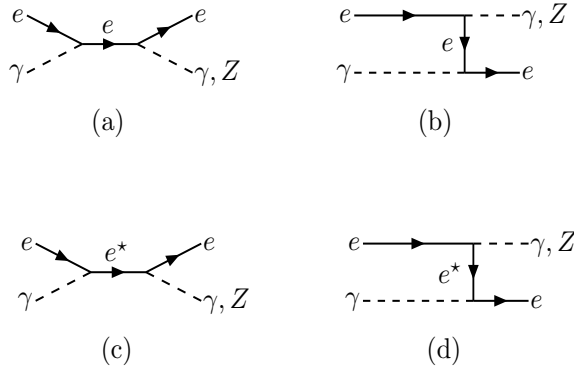


FIG. 2. Diagrams for the process  $e\gamma \rightarrow e\gamma, eZ$ .



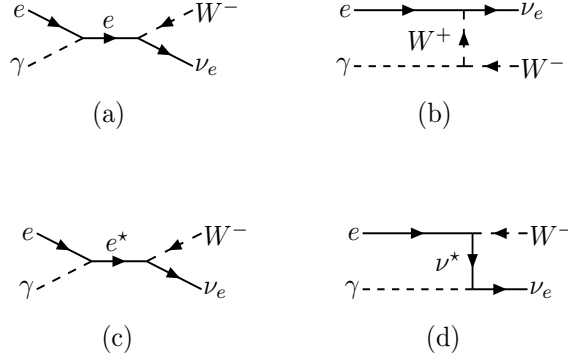


FIG. 3. Diagrams for the process  $e\gamma \rightarrow \nu_e W^-$ .

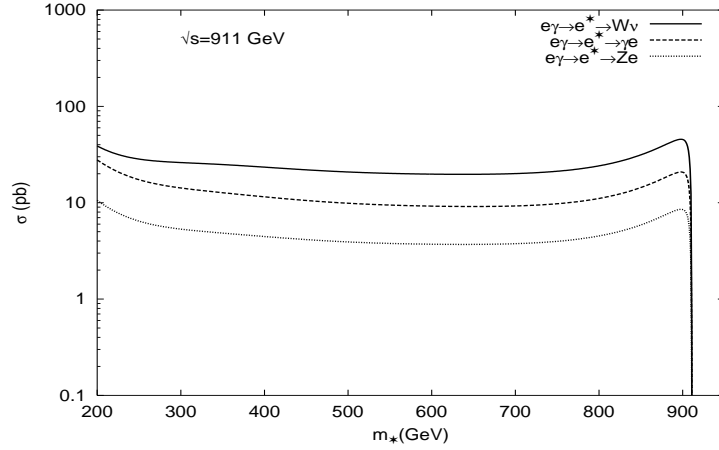


FIG. 4. The production cross sections of excited electron depending on its mass in three different channels at TESLA and CLIC based  $e\gamma$  colliders with  $\sqrt{s} = 911$  GeV.

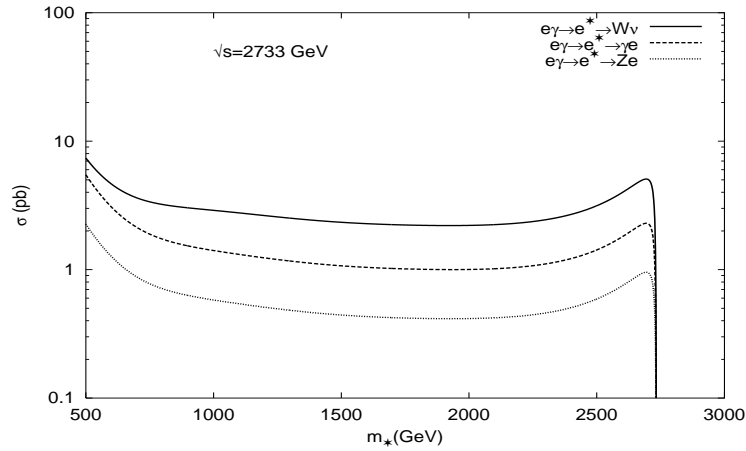


FIG. 5. The cross sections for excited electron production at CLIC based  $e\gamma$  colliders with  $\sqrt{s} = 2733$  GeV.

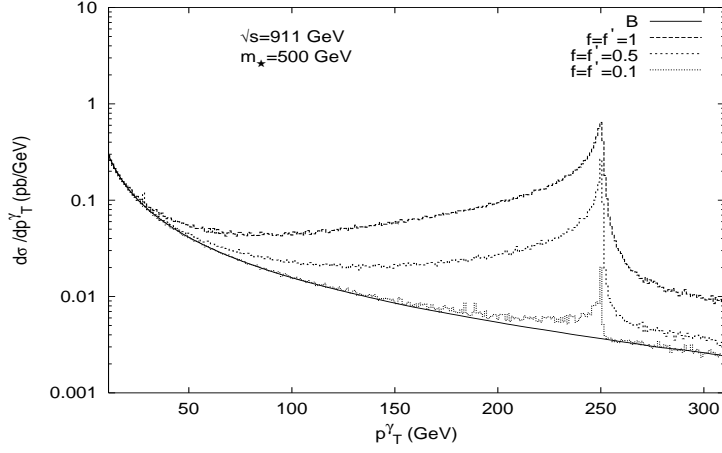


FIG. 6. Transverse momentum distribution of photon for  $e\gamma \rightarrow e\gamma$  process according to different couplings  $f = f'$  for  $m_* = 500$  GeV at TESLA based  $e\gamma$  collider with  $\sqrt{s} = 911$  GeV.

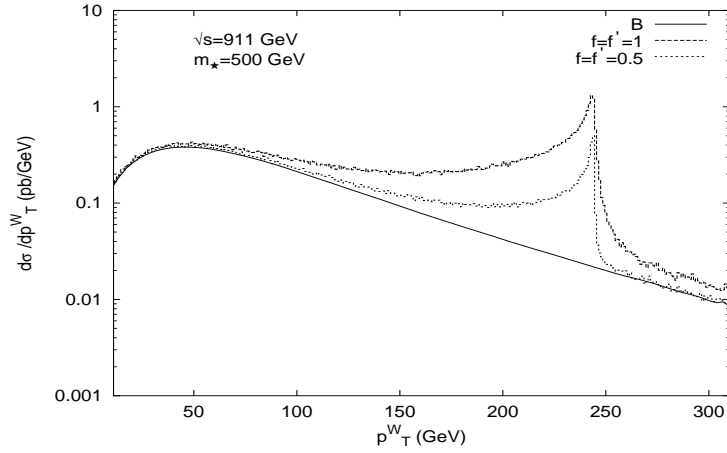


FIG. 7. Transverse momentum distribution of W boson for  $e\gamma \rightarrow \nu W$  process according to different couplings  $f = f'$  for  $m_* = 500$  GeV at TESLA based  $e\gamma$  collider with  $\sqrt{s} = 911$  GeV.

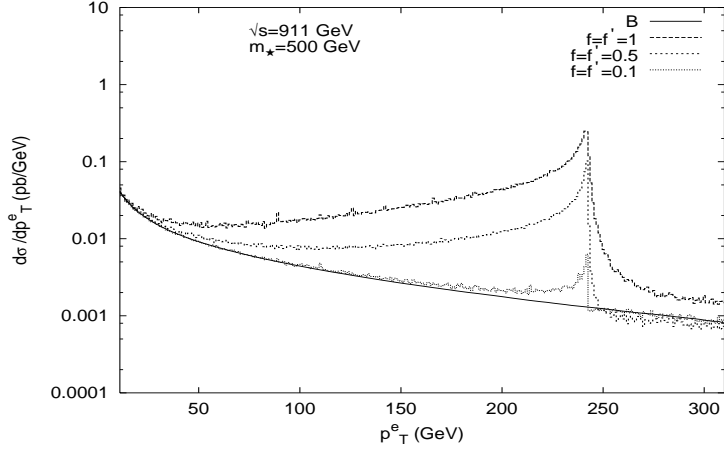


FIG. 8. Transverse momentum distribution of electron for  $e\gamma \rightarrow eZ$  process according to different couplings  $f = f'$  for  $m_* = 500 \text{ GeV}$  at TESLA based  $e\gamma$  collider with  $\sqrt{s} = 911 \text{ GeV}$ .